Hindawi
Scientific Programming
Volume 2021, Article ID 9629884, 7 pages
https://doi.org/10.1155/2021/9629884

Research Article

Extreme Learning Machine Denoising Algorithm Based Analysis of Transvaginal 3-Dimensional Ultrasonic Image for the Diagnostic Effect of Intrauterine Adhesion

Jing Wu and Zhikun Zhang

Department of Ultrasound, Tianjin Central Hospital of Gynecology Obstetrics, Tianjin 300100, China

Correspondence should be addressed to Zhikun Zhang; 201771107@yangtzeu.edu.cn

Received 17 June 2021; Revised 12 July 2021; Accepted 23 July 2021; Published 3 August 2021

Academic Editor: Gustavo Ramirez

The aim was to analyze the application values and diagnostic effects of transvaginal 3-dimensional (3D) ultrasonic image based on extreme learning machine denoising algorithm (ELMDA) in the diagnosis of intrauterine adhesions (IUA). The speckle noise in the 3D ultrasound image was removed with the ELMDA. Its peak signal-to-noise ratio (PSNR) and the mean square error (MSE) were compared with those of the median filter algorithm (MFA) with the anisotropic diffusion algorithm (ADA) and wavelet threshold. The ELMDA was used in the diagnosis of 3D ultrasound images to compare the accuracy of hysteroscopy with transvaginal 3D ultrasound and two-dimensional (2D) ultrasound in the diagnosis of IUA. The results showed that the MSE of ELMDA was dramatically smaller than those of ADA and WT-MFA and its PSNR was higher than those of the other two algorithms ($P < 0.05$) when the noise variance was constant. The diagnostic accuracy of mild and moderate adhesions by 2D ultrasound was statistically different ($P < 0.05$) compared with hysteroscopy. But the diagnosis results of severe adhesions were consistent, and the diagnosed cases were both 6 (11.11%) with no statistical difference ($P > 0.05$). In addition, there was no statistically great difference in the diagnostic accuracy of IUA by transvaginal 3D ultrasound and hysteroscopy ($P > 0.05$), and the diagnosis results of moderate and severe adhesions were consistent (both 20 cases (37.04%) and 6 cases (11.11%), respectively) with no statistical difference ($P > 0.05$). The diagnostic accuracy of 3D ultrasound was 96.30%, while that of 2D ultrasound was 90.74%, showing a statistical difference ($P < 0.05$). In conclusion, ELMDA had a good effect of denoising, and there was a high accuracy of the application of 3D transvaginal ultrasound to diagnose IUA, which had reliable clinical application value.

1. Introduction

IUA is also known as Asherman's syndrome [1]. IUA is one of the common gynecological diseases with a high clinical incidence. This is because multiple factors result in damage of the endometrial basement layer to cause the adhesions of cervical canal or uterine muscle for partial or total occlusion of the uterine cavity, thereby emerging with menstrual abnormalities, infertility, and repeated abortion in patients [2, 3]. In recent years, the incidence of IUA has kept rising with the increase of abortion rate, which has become the second major cause of secondary infertility after fallopian tube factors, posing a serious threat to women's health [4, 5]. Hysteroscopy is currently an effective operation for the treatment of IUA and the gold standard for diagnosis [6]. The commonly used hysteroscopy and hysterography are both invasive examinations, and transvaginal 2D ultrasound examination also has certain limitations so that the diagnostic accuracy of IUA is low [7, 8].

With the continuous development of ultrasound technology and the improvement of the instrument resolution, 3D transvaginal sonograph (3D-TVS) has made up for the defects of 2D ultrasound and has become a new method for clinical diagnosis of IUA [9]. Ahmadi et al. [10] indicated that 3D contrast-enhanced ultrasonography for uterine cavity was a minimally invasive and cost-effective means to explore the adhesions. However, 3D ultrasonic images are directly reconstructed based on the 2D ultrasonic images

obtained by scanning, which contain more speckle noises, so the image quality degrades, and the reconstruction accuracy is not high. Extreme learning machine (ELM) is a new and easy-to-use single-hidden-layer feed-forward neural network learning algorithm, which can randomly assign the input weight and offset of hidden layer during algorithm execution to generate the unique optimal solution [11, 12]. ELM has fast learning speed and good generalization performance. Therefore, ELMDA can be applied to remove speckle noises in the image to ensure the effectiveness and accuracy of 3D ultrasonic image reconstruction.

In summary, IUA, as a common cause of infertility, amenorrhea, and repeated abortion, seriously endangers women's reproductive health. The transvaginal 3D ultrasonic examination can clarify the actual situation of IUA to improve the clinical diagnosis and treatment. But the reconstructed 3D ultrasonic image contains speckle noises, and ELMDA can remove speckle noises, making the 3D ultrasonic image more accurate. Therefore, the transvaginal 3D ultrasound based on ELMDA was employed to promote the diagnostic accuracy of IUA, and the clinical application value of this transvaginal 3D ultrasound was discussed in the diagnosis of IUA.

2. Materials and Methods

2.1. Research Objects. 54 patients with IUA who admitted to the hospital from February 2019 to January 2020 were selected as the research objects. Their age ranged from 20 to 45 years with an average age of 36.31 ± 2.25 years. The experiment had been approved by the Medical Ethics Committee of the hospital. The patients and their family members had been informed of the experiment and signed the informed consent.

The criteria for inclusion were defined to include patients who were above 20 years of age, were diagnosed as IUA, had complete preoperative ultrasound examination data, should receive the hysteroscopic treatment, were in good health, and could normally cooperate with the experiment to receive treatment.

The criteria for exclusion were defined to include patients who had uncertain preoperative diagnosis, suffered from uterine polyps and submucosal fibroids, had incomplete clinical data, and dropped out of the experiment due to their own reasons.

2.2. Extreme Learning Machine Denoising Algorithm. The key of ELMDA was to calculate the output weight and determine the learning mathematical model based on the given activation function type and the number of hidden nodes.

Assuming that there were M arbitrary samples (a_i, b_i) ($\mathrm{a_i} = [\mathrm{a_{i1}}, \mathrm{a_{i2}}, \cdots \mathrm{a_{im}}]^B \in R^m$ and $b_\mathrm{i} = [b_{\mathrm{i}1}, \mathrm{b_{i2}}, \cdots \mathrm{b_{im}}]^B \in R^n$), the single-hidden-layer feed-forward neural network contained T nodes of hidden layer that could be expressed as in the following equation:

$$\sum_{i=1}^{T} \beta_i f_i\left(x_j\right) = \sum_{i=1}^{T} \beta_i f\left(z_i \cdot x_j + y_i\right) = q_j, \quad j = 1, 2, \ldots, M. \tag{1}$$

In equation (1), $f(x)$ represented the activation function, which could generally be chosen as sine function, hyperbolic function, or radial basis function. $z_i = [z_{i1}, z_{i2}, \ldots, z_{im}]^B$ stood for the weight vector that connected the input data with i^{th} nodes of hidden layer, $\beta_i = [\beta_{i1}, \beta_{i2}, \ldots, \beta_{\mathrm{in}}]^B$ expressed the weight vector connected the output data and the i^{th} node of hidden layer, y_i stood for the offset of the i^{th} hidden layer node, q_j referred to the feed-forward neural network (FNN) of single hidden layer, and $z_i\, x_i$ represented the inner product of vector. The objective of the single-hidden-layer feed-forward neural network was to obtain the minimum output error, as shown in the following equation:

$$\sum_{j=1}^{T} \left\| q_j - b_j \right\| = 0. \tag{2}$$

Therefore, β_i, z_i, and x_i existed and could be calculated in the following equation:

$$\sum_{i=1}^{T} \beta_i f\left(z_i \cdot x_j + y_i\right) = b_j, \quad j = 1, 2, \ldots, M. \tag{3}$$

The above equation could be expressed by a matrix as follows:

$$H\beta = B. \tag{4}$$

In equation (4), H, β, and B represented the output matrix of the hidden layer, the output weight of the hidden layer, and the expected output matrix, respectively. In addition, they could be expressed as in the three following equations:

$$H = H\left(z_1, \cdots, z_T, y_1, \cdots, y_T, x_1, \cdots, x_M\right), \tag{5}$$

$$H = \begin{bmatrix} f\left(z_1 \cdot x_1 + y_1\right) \ldots \left(z_t \cdot x_1 + y_T\right) \\ f\left(z_1 \cdot x_M + y_1\right) \ldots f\left(z_t \cdot x_M + y_T\right) \end{bmatrix}_{M \times T}, \tag{6}$$

$$\begin{aligned} \beta &= \begin{bmatrix} \beta_1^B \\ \vdots \\ \beta_T^B \end{bmatrix}_{T \times n}, \\ B &= \begin{bmatrix} b_1^B \\ \vdots \\ b_M^B \end{bmatrix}_{M \times n}. \end{aligned} \tag{7}$$

If the input weight zi and offset yi of the hidden layer were set in ELMDA, the output matrix H of the hidden layer could be uniquely determined. The training process of the single-hidden-layer feed-forward neural network could be transformed into solving a linear system $H\beta = B$, and then the output weight β could be determined.

$$\widehat{\beta} = H^{\dagger} B. \tag{8}$$

In equation (8), $H^{\dagger}$ expressed the generalized inverse of matrix H, and it could be proved that the norm obtained was the smallest and unique.

ELMDA was used for image denoising, which should be divided into two steps (training stage and testing stage). In this study, sigmoid function was selected as the activation function of ELMDA. The number of nodes in the hidden layer was set to 120, so PSNR of the image was the largest and the denoising effect was the best. The image denoising process of ELMDA is shown in Figure 1.

2.3. Evaluation Indexes of Speckle Noise Removal Effect of Three Algorithms. ADA and WT-MFA were common ultrasound image denoising methods. In order to detect the denoising effect of different algorithms, ADA [13], WT-MFA [14], and ELMDA were employed to detect the image containing speckle noises, and the parameters of the three algorithms were set at the values that achieved the best effect. The denoising results were quantitatively analyzed by comparing the PSNR and MSE of the denoised images.

2.4. Examination Method of Intrauterine Adhesions. The method of transvaginal 2D ultrasound examination was as follows. First, the patients were told to empty the bladder before examination, and the cystolithotomy position was taken on the examination bed. Second, the iodophor cotton balls were applied to disinfect the vaginal scanning probe, the condom was placed on the probe, and the coupling agent was applied. Third, the operator put the probe into the vaginal area of the patient slowly with disposable gloves. Fourth, there was a comprehensive scanning of the uterus by tilting and rotating to observe its size, shape, and uterine cavity. Fifth, each uterine meridian and endometrial thickness were recorded, and the endometrial morphology, echo, and presence of endometrial blood flow were observed and recorded in detail.

The transvaginal 3D ultrasound examination method contained the following steps. The 3D ultrasound examination was adopted after the 2D ultrasound examination. The volume and size of the sampling frame should be adjusted based on the specific needs. The patient should be told that she held her breath, and then 3D data acquisition system was started to collect data of uterus and endometrium. The three axes were adjusted to choose the best observation direction so as to get a clear uterine coronal plane 3D image. Then, the changes of uterine cavity morphology, endometrial thickness, and echo were observed and recorded.

Hysteroscopy examination contained the following steps: All patients underwent hysteroscopy. The cystolithotomy position was taken on the examination bed, the cervical tube was disinfected, and cotton swabs were adopted to dip 2% lidocaine for anesthesia of the cervical canal. 5% glucose was added as a distending medium and was put gently in the hysteroscopy so as to observe the condition of cervical tube. The condition, scope, and degree of IUA were recorded, the adhesion sites were separated for the patients with IUA, and antibiotics were given to prevent infection after the surgery.

2.5. Classification Standard of Intrauterine Adhesions. According to relevant studies, ultrasonic diagnosis results of IUA were mild, moderate, and severe, respectively. Mild adhesions meant that the endometrial thickness was greater than 5 mm, its range was less than 1/4 of the length of uterine cavity, and the opening of fallopian tube was normal or the lesion was mild. The moderate adhesions of 1/4 to 3/4 were involved, the opening of fallopian tube was abnormal, and some of the uterine cavity was blocked. The severe adhesions were that endometrial thickness was less than 2 mm (extremely narrow), uterine walls were adhered or the adhesion zone was hypertrophic, and the range was larger than 3/4 of the length diameter of uterine cavity. Besides, some patients had the uterine cavity completely locked.

2.6. Statistical Methods. SPSS 19.0 statistical software was used for data processing in this study, and the measurement data could be expressed as mean ± standard deviation ($\bar{x} \pm s$). In addition, count data was represented by percentage (%). The analysis of variance was used for pairwise comparison. $P < 0.05$ meant that the results were statistically significant.

3. Results

3.1. The Effects of Three Algorithms to Remove Speckle Noise. For quantitative analysis of denoising results, MSE and PSNR of denoised images were considered as quantitative indexes. Speckle noises with variances of 0.1, 0.5, and 1.0 were added to the original image in sequence, and the test results were recorded in time. The results showed that the denoising MSE of ADA were 0.0096, 0.0121, and 0.0139 when the noise variances were 0.1, 0.5, and 1.0, respectively. The denoising MSE of different noise variances in WT-MFA were 0.0032, 0.0087, and 0.0135, respectively. The denoising MSE of ELMDA used in this study were 0.0022, 0.0039, and 0.0071 when the noise variances were 0.1, 0.5, and 1.0, respectively. As shown in Figure 2, the MSE of ELMDA was greatly smaller than those of ADA and WT-MFA when the noise variance was constant, showing a statistical difference ($P < 0.05$). When the noise variance increased, the MSE of the three algorithms all grew but the MSE of ELMDA was still the minimum.

When the noise variances were 0.1, 0.5, and 1.0, the PSNR of ADA was 67.53, 66.49, and 65.98 in sequence; the PSNR of WT-MFA was 71.26, 67.54, and 65.87, respectively; and the PSNR of ELMDA was 74.08, 71.12, and 69.57, respectively. Figure 3 indicates that the PSNR of ELMDA was higher than those of ADA and WT-MFA when the noise variance was constant, and the difference was statistically obvious ($P < 0.05$). With the increase of noise variances, the PSNR of the three algorithms decreased, while the PSNR of ELMDA was still the largest.

3.2. Hysteroscopy Results of Patients with Intrauterine Adhesions. In this study, 54 patients with IUA were examined by hysteroscopy and all of them were diagnosed with IUA: 28 patients with mild adhesions (51.85%), 20 patients with moderate adhesions (37.04%), and 6 patients with severe adhesions (11.11%) (Figure 4).

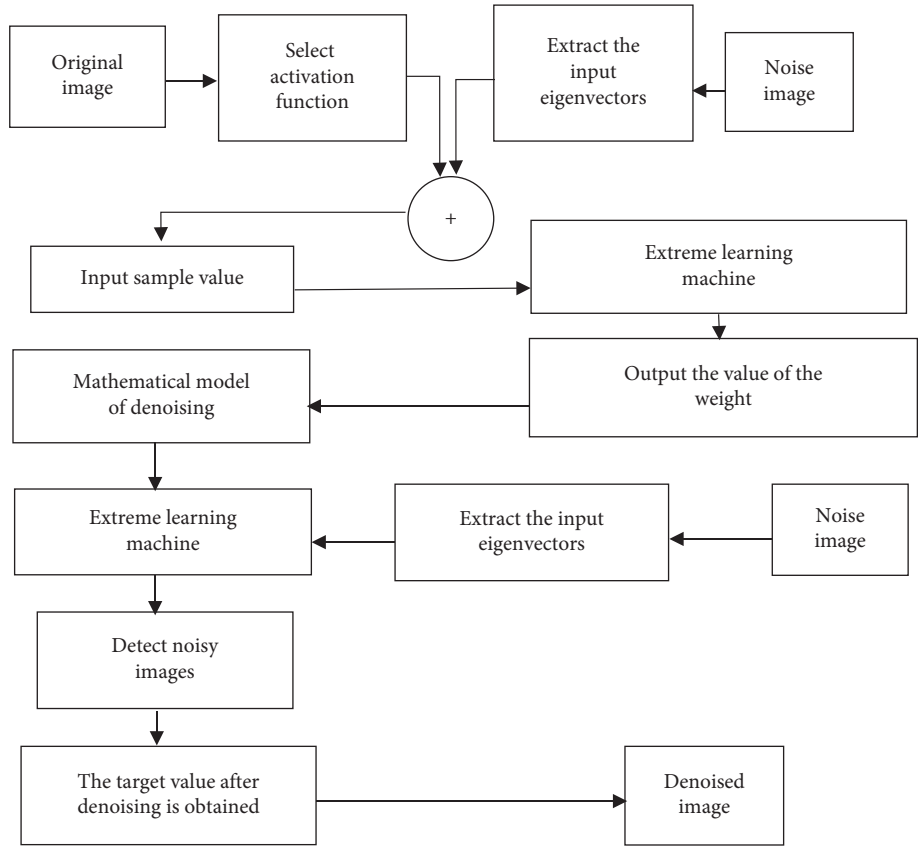

Figure 1: The process of ELMDA.

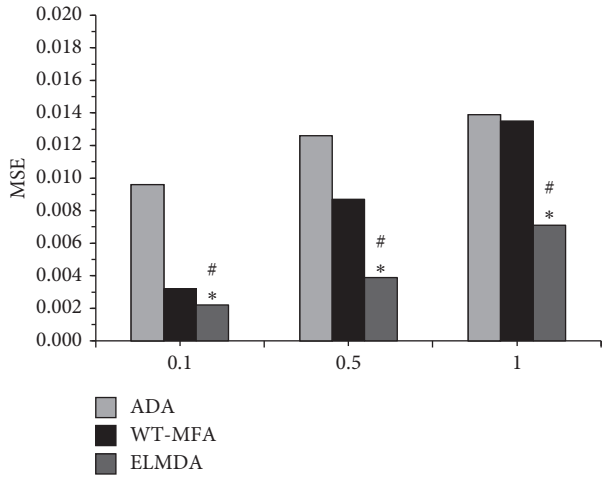

Figure 2: Comparison of MSE in the three algorithms with different noise variances. * indicates that there was a statistically obvious difference compared with WT-MFA ($P < 0.05$); and # indicates that the difference was statistically substantial compared to ADA ($P < 0.05$).

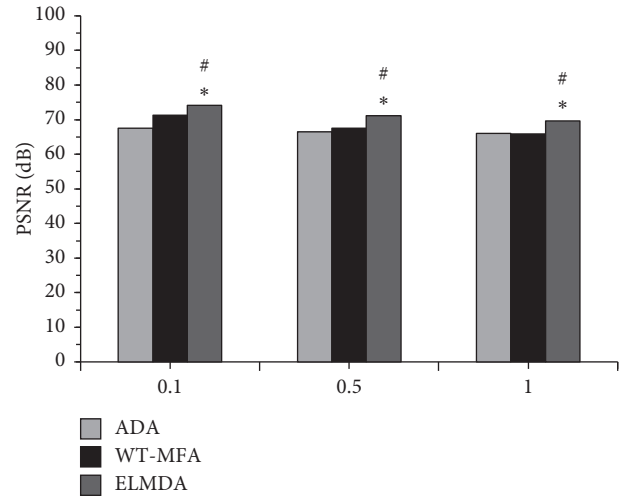

Figure 3: Comparison of PSNR in the three algorithms with different noise variances. *indicates that the difference was statistically substantial in contrast to WT-MFA ($P < 0.05$); and # reveals that there was a statistically great difference compared to ADA ($P < 0.05$).

3.3. Diagnostic Results of Transvaginal 2-Dimensional Ultrasound Examination. There were 31 patients with mild adhesions (57.41%) detected by transvaginal 2D ultrasound examination. 12 patients suffered from moderate adhesions, accounting for 22.22%. Besides, 6 patients were diagnosed with severe adhesions, accounting for 11.11%. There were 5 patients with no adhesions (9.26%). As shown in Figure 5, the diagnostic rate of 2D ultrasound examination for mild adhesions was higher than that of hysteroscopy by comparison with the diagnosis results of 2D ultrasound examination and hysteroscopy, with statistically huge difference ($P < 0.05$). The diagnostic rate of 2D ultrasound examination

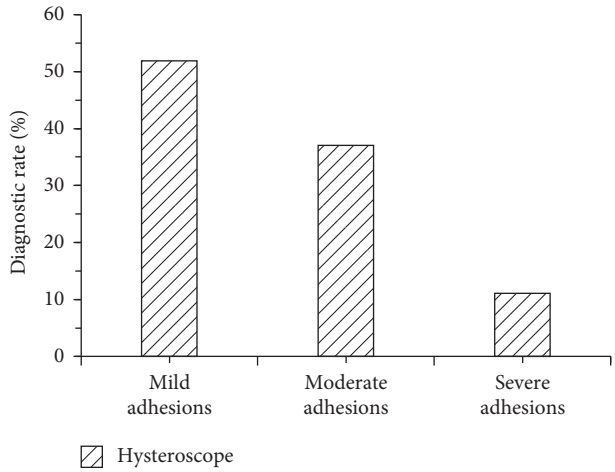

Figure 4: Hysteroscopy diagnostic results of patients with IUA.

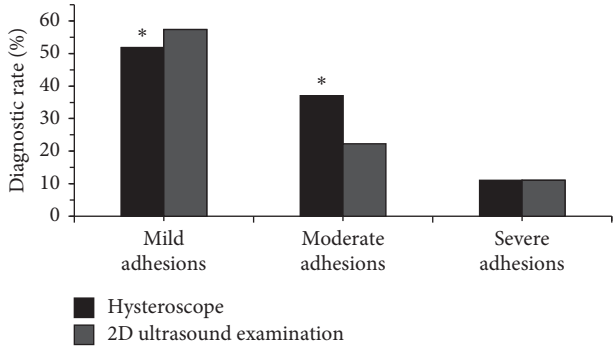

Figure 5: Comparison of diagnosis results between 2D ultrasound examination and hysteroscopy. * shows that the difference was statistically obvious in contrast to hysteroscopy ($P < 0.05$).

for moderate adhesions was lower than that of hysteroscopy, and the difference was statistically remarkable ($P < 0.05$). However, there was no statistical difference in the diagnosis of severe adhesions ($P > 0.05$).

3.4. Diagnostic Results of Transvaginal 3-Dimensional Ultrasound Examination. According to the features of transvaginal 3D ultrasound images, 26 of the 54 patients presented mild adhesions (48.15%), 20 moderate adhesions (37.04%), 6 severe adhesions (11.11%), and 2 no adhesions (3.70%). Figure 6 reveals that the diagnostic results of transvaginal 3D ultrasound examination for moderate and severe adhesions were consistent with the results of hysteroscopy, and there was no obvious difference between two diagnoses of mild adhesions ($P > 0.05$), so the diagnostic rates of transvaginal 3D ultrasound examination and hysteroscopy were not statistically different ($P > 0.05$). Figure 7 shows the 2D and 3D ultrasound images of one female patient with mild IUA (aged 31 years).

3.5. Comparison of Diagnosis Results between Transvaginal 3-Dimensional and 2-Dimensional Ultrasound Examinations. There was a comparison of diagnostic results of transvaginal 3D and 2D ultrasound examinations. Based on the above

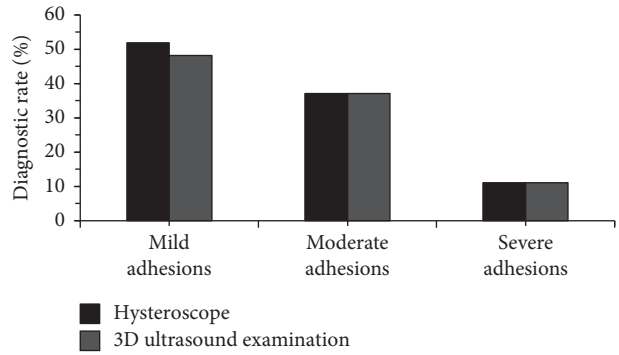

Figure 6: Comparison of diagnosis results between 3D ultrasound examination and hysteroscopy.

results, the diagnostic rate of 2D ultrasound examination was 90.74%, while that of 3D ultrasound examination was 96.30%. As shown in Figure 8, the overall diagnostic rate of 3D ultrasound examination in diagnosing IUA was markedly higher than that of 2D ultrasound examination, with statistical substantial difference ($P < 0.05$). The results of transvaginal 3D ultrasound examination in the diagnosis of mild and moderate adhesions were better than those of 2D ultrasound examination ($P < 0.05$), which were closer to the diagnosis results of hysteroscopy. The results of 2D and 3D ultrasonic diagnosis of severe adhesions were consistent with no statistical difference ($P > 0.05$), which were also in accordance with those of hysteroscopy.

4. Discussion

As a common gynecological disease, IUA seriously endangers women's health and is also a crucial cause of female infertility. Some patients also suffer from repeated abortion, ectopic pregnancy, and stillbirth [15, 16]. At present, the main methods to diagnose IUA are transvaginal 2D ultrasound examination, X-ray hysterosalpingography, and hysteroscopy. Among them, hysteroscopy and X-ray hysterosalpingography are both invasive examinations. The traditional transvaginal 2D ultrasound examination is difficult to determine the accurate location of endometrial lesions, and the diagnosis accuracy of IUA is low. In recent years, the emergence of transvaginal 3D ultrasound examination makes up for the deficiency of 2D ultrasound examination and becomes a new method for the diagnosis of IUA [17, 18]. The transvaginal 3D ultrasound examination is reconstructed on the basis of 2D ultrasound examination and contains speckle noises, which makes the image precision not enough.

Aiming at the speckle noises in ultrasonic images, ELMDA was adopted in this study and there was a comparison of denoising performance of three different algorithms. Besides, ELMDA was applied to 3D ultrasound examination to diagnose IUA and its results were compared with those of hysteroscopy and transvaginal 2D ultrasound examination. The final results revealed that MSE of ELMDA was dramatically smaller than those of ADA and WT-MFA, and the difference was statistically obvious ($P < 0.05$).

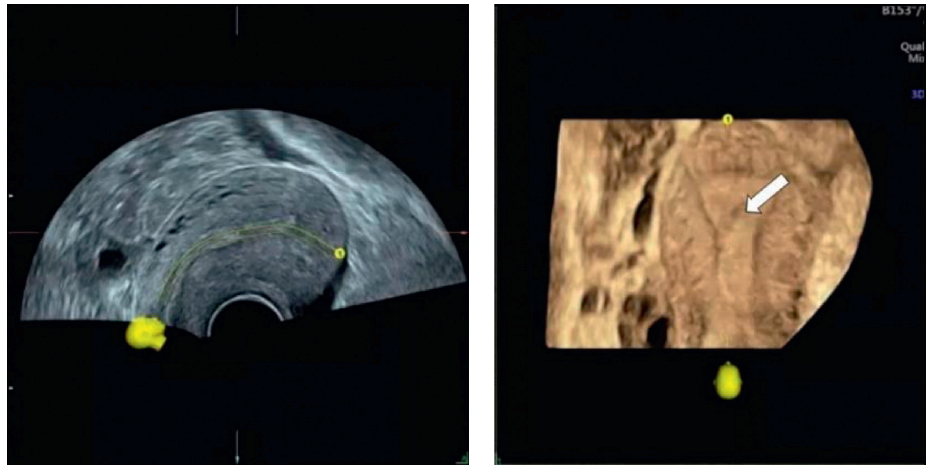

(a) (b)

Figure 7: 2D and 3D ultrasound images of one female patient with mild IUA (aged 31 years). A is the transvaginal 2D ultrasound image, showing slight endometrial irregularities; and B is the transvaginal 3D ultrasound image with the arrow pointing to the defect.

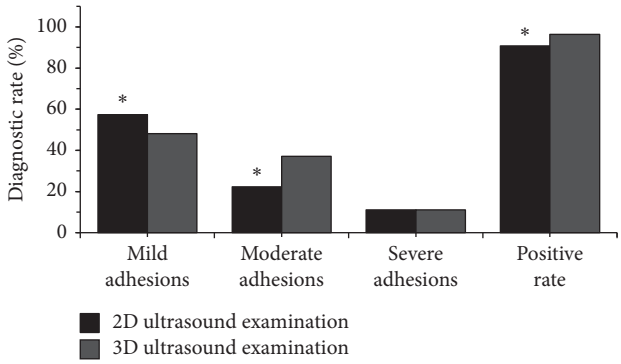

Figure 8: Comparison of diagnosis results between 2D and 3D ultrasound examinations. * expresses that the difference in diagnostic rate was statistically considerable compared with 2D ultrasound examination ($P < 0.05$).

Moreover, ELMDA had a higher PSNR than those of ADA and WT-MFA when the noise variance was constant, showing a statistically marked difference ($P < 0.05$). ELMDA had a better denoising effect, which was different from the research results of Usha et al. [19] due to the fact that the sample size was too small and the included objects were different. The results of hysteroscopy were regarded as the criteria for the diagnosis of IUA, and the results of transvaginal 2D and 3D ultrasound examinations were compared. The results indicated that the diagnostic rate of transvaginal 2D ultrasound examination for mild and moderate adhesions was statistically different compared to that of hysteroscopy ($P < 0.05$). However, the diagnosis results of severe adhesions were consistent, with 6 (11.11%) cases diagnosed ($P > 0.05$). What is more, there was no statistically great difference in the diagnosis rate of IUA between transvaginal 3D ultrasound examination and hysteroscopy ($P > 0.05$), and the diagnosis results of moderate and severe adhesions were the same (both 20 cases (37.04%) and 6 cases (11.11%)), with no statistically significant difference ($P > 0.05$). The diagnostic accuracy of 3D ultrasound examination was 96.30%, while that of 2D ultrasound examination was 90.74%. Thus, the diagnostic accuracy of transvaginal 3D ultrasound examination for IUA was remarkably higher than that of 2D ultrasound examination, with statistical difference ($P < 0.05$). This was similar to the research results of Kim et al. [20], both of which suggested that 3D ultrasound examination could be employed to diagnose IUA with high diagnostic accuracy.

5. Conclusion

ELMDA was applied to denoise the speckle noises in images based on 3D ultrasound examination and was compared with ADA and WT-MFA. Moreover, ELMDA was used for 3D ultrasound image diagnosis so as to explore the diagnostic accuracy of 3D ultrasound examination based on ELMDA. The results showed that ELMDA had the lowest MSE and the highest PSNR with better denoising effect. In addition, transvaginal 3D ultrasound examination after denoising had a high accuracy in diagnosing IUA, which was superior to transvaginal 2D ultrasound examination, and had certain clinical application value. However, the small sample size of the patients selected in this study might cause a reliable deviation in the results. In the future, the selection range of patients should be increased to further explore the effective rate of transvaginal 3D ultrasound examination in the diagnosis of IUA. To sum up, the results of this study provided a theoretical basis for the investigation of ELMDA and the application of transvaginal 3D ultrasound examination in the diagnosis of IUA.

Data Availability

The data used to support the findings of this study are available from the corresponding author upon request.

Conflicts of Interest

The authors declare no conflicts of interest.

References

[1] M. W. Healy, B. Schexnayder, M. T. Connell et al., "Intrauterine adhesion prevention after hysteroscopy: a systematic review and meta-analysis," *American Journal of Obstetrics and Gynecology*, vol. 215, no. 3, pp. 267–275, 2016.

[2] H.-Y. Zhu, T.-X. Ge, Y.-B. Pan, and S.-Y. Zhang, "Advanced role of hippo signaling in endometrial fibrosis," *Chinese Medical Journal*, vol. 130, no. 22, pp. 2732–2737, 2017.

[3] Z. Fei, Z. Bin, X. Xin, H. Fei, and C. Yuechong, "Meta-analysis on the use of hyaluronic acid gel to prevent recurrence of intrauterine adhesion after hysteroscopic adhesiolysis," *Taiwanese Journal of Obstetrics & Gynecology*, vol. 58, no. 6, pp. 731–736, 2019.

[4] Z. Khan and J. M. Goldberg, "Hysteroscopic management of a's syndrome," *Journal of Minimally Invasive Gynecology*, vol. 25, no. 2, pp. 218–228, 2018.

[5] A. Di Spiezio Sardo, G. Calagna, M. Scognamiglio et al., "Prevention of intrauterine post-surgical adhesions in hysteroscopy: a systematic review," *European Journal of Obstetrics & Gynecology and Reproductive Biology*, vol. 203, pp. 182–192, 2016.

[6] R. Deans, T. Vancaillie, W. Ledger, J. Liu, and J. A. Abbott, "Live birth rate and obstetric complications following the hysteroscopic management of intrauterine adhesions including Asherman syndrome," *Human Reproduction*, vol. 33, no. 10, pp. 1847–1853, 2018.

[7] L. Su, L. You, and H. P. Huang, "Risk factors of intrauterine adhesion after hysteroscopic resection of endometrial polyps," *Zhongguo Yi Xue Ke Xue Yuan Xue Bao*, vol. 39, no. 6, pp. 812–816, 2017.

[8] M. J. Liu, Z. F. Liu, W. H. Yin, X.-R. Chen, L. Gao, and H.-J. Sun, "Application of transvaginal three-dimensional power Doppler ultrasound in benign and malignant endometrial diseases," *Medicine (Baltimore)*, vol. 98, no. 46, Article ID e17965, 2019.

[9] A. Burjoo, X. Zhao, L. Zou et al., "The role of preoperative 3D-ultrasound in intraoperative judgement for hysteroscopic adhesiolysis," *Annals of Translational Medicine*, vol. 8, no. 4, p. 55, 2020.

[10] F. Ahmadi and M. Javam, "Role of 3D sonohysterography in the investigation of uterine synechiae/Asherman's syndrome: pictorial assay," *Journal of Medical Imaging and Radiation Oncology*, vol. 58, no. 2, pp. 199–202, 2014.

[11] E. Dreisler and J. J. Kjer, "Asherman's syndrome: current perspectives on diagnosis and management," *International Journal of Women's Health*, vol. 11, pp. 191–198, 2019.

[12] X. X. Yin, Y. Zhang, J. Cao, J.-L. Wu, and S. Hadjiloucas, "Exploring the complementarity of THz pulse imaging and DCE-MRIs: toward a unified multi-channel classification and a deep learning framework," *Computer Methods and Programs in Biomedicine*, vol. 137, pp. 87–114, 2016.

[13] H. Choi and J. Jeong, "Speckle noise reduction for ultrasound images by using speckle reducing anisotropic diffusion and Bayes threshold," *Journal of X-Ray Science and Technology*, vol. 27, no. 5, pp. 885–898, 2019.

[14] J. F. Al-Asad, A. H. Khan, G. Latif, and W. Hajji, "QR based despeckling approach for medical ultrasound images," *Current Medical Imaging Reviews*, vol. 15, no. 7, pp. 679–688, 2019.

[15] Y. Chi, P. He, L. Lei et al., "Transdermal estrogen gel and oral aspirin combination therapy improves fertility prognosis via the promotion of endometrial receptivity in moderate to severe intrauterine adhesion," *Molecular Medicine Reports*, vol. 17, no. 5, pp. 6337–6344, 2018.

[16] C. S. Chiu, Y. M. Hwu, R. K. Lee et al., "Intrauterine adhesion prevention with Malecot catheter after hysteroscopic myomectomy: a novel approach," *Taiwanese Journal of Obstetrics & Gynecology*, vol. 59, no. 1, pp. 56–60, 2020.

[17] C. Apirakviriya, T. Rungruxsirivorn, V. Phupong et al., "Diagnostic accuracy of 3D-transvaginal ultrasound in detecting uterine cavity abnormalities in infertile patients as compared with hysteroscopy," *European Journal of Obstetrics & Gynecology and Reproductive Biology*, vol. 200, pp. 24–28, 2016.

[18] L. Yan, A. Wang, R. Bai et al., "Application of SonoVue combined with three-dimensional color power angiography in the diagnosis and prognosis evaluation of intrauterine adhesion," *European Journal of Obstetrics & Gynecology and Reproductive Biology*, vol. 198, pp. 68–72, 2016.

[19] A. Usha, N. Shajil, and M. Sasikala, "Automatic anisotropic diffusion filtering and graph-search segmentation of macular spectral-domain optical coherence tomographic (SD-OCT) images," *Current Medical Imaging Reviews*, vol. 15, no. 3, pp. 308–318, 2019.

[20] M. J. Kim, Y. Lee, C. Lee et al., "Accuracy of three dimensional ultrasound and treatment outcomes of intrauterine adhesion in infertile women," *Taiwanese Journal of Obstetrics & Gynecology*, vol. 54, no. 6, pp. 737–741, 2015.